ADVANCED ENERGY MATERIALS

Supporting Information

for *Adv. Energy Mater.,* DOI: 10.1002/aenm.202000142

Flexible Pseudocapacitive Electrochromics via Inkjet Printing of Additive-Free Tungsten Oxide Nanocrystal Ink

Long Zhang, Dongliang Chao, Peihua Yang, Louis Weber, Jia Li, Tobias Kraus,* and Hong Jin Fan**

Supporting Information

Flexible Pseudocapacitive Electrochromics via Inkjet Printing of Additive-Free Tungsten Oxide Nanocrystal Ink

Long Zhang, Dongliang Chao, Peihua Yang, Louis Weber, Jia Li, Tobias Kraus,* and Hong Jin Fan**

L. Zhang, Dr. P. Yang, L. Weber, Prof. Dr. T. Kraus
INM - Leibniz Institute for New Materials, Campus D2 2, 66123 Saarbrücken, Germany
E-mail: tobias.kraus@leibniz-inm.de

Dr. D. Chao, Dr. P. Yang, Prof. Dr. H. J. Fan
School of Physical and Mathematical Sciences, Innovative Centre for Flexible Devices, Nanyang Technological University, Singapore, 637371 Singapore
E-mail: peihua.yang@ntu.edu.sg; fanhj@ntu.edu.sg

Dr. J. Li
Rolls-Royce@NTU Corporate Lab, Nanyang Technological University, Singapore, 639798 Singapore

Prof. Dr. K. Tobias
Colloid and Interface Chemistry, Saarland University, 66123 Saarbrücken, Germany

Keywords: inkjet printing, flexible electrochromics, pseudocapacitive zinc-ion storage, tungsten oxide, additive-free nanocrystals ink

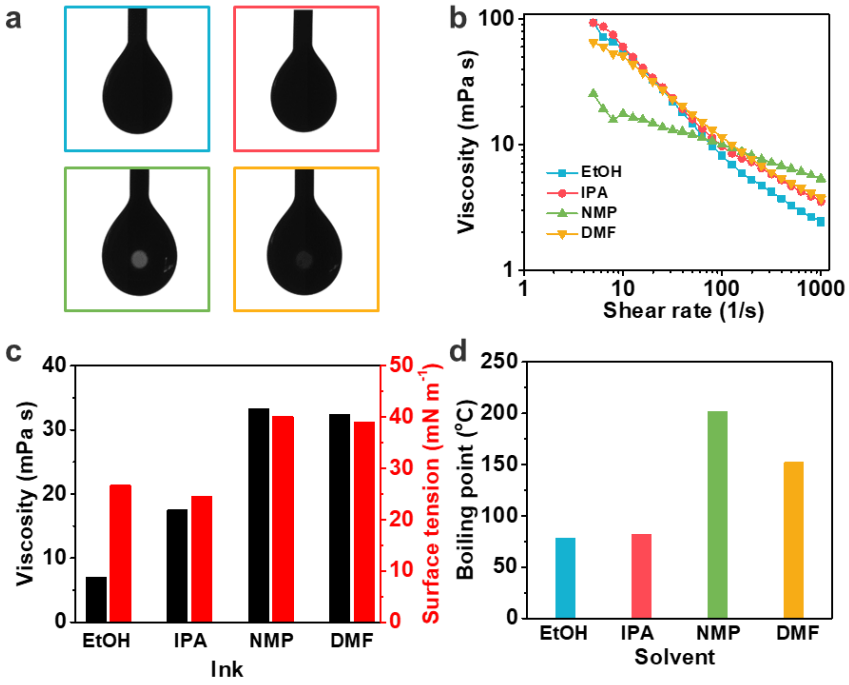

Figure S1. Inks properties. (a) Surface tensions of inks with different solvents. (b) The viscosity of WO_{3-x} inks plotted as a function of shear rate. (c) Viscosity and surface tension collection. (d) The boiling point of the solvents applied in inks formulation. The nozzle blocking phenomenon is not easy to happen during the printing process using NMP ink, as NMP gives the highest boiling point value (over 200 °C).

Table S1. Fluidic properties of WO_{3-x} inks.

Ink	Density ($g\ cm^{-3}$)	Viscosity (mPa s)	Surface tension ($mN\ m^{-1}$)	*Z* value
EtOH	0.89	7.0	26.7	3.3
IPA	0.89	17.5	24.5	1.2
NMP	1.13	30.0	40.1	1.1
DMF	1.04	32.4	39.1	0.9

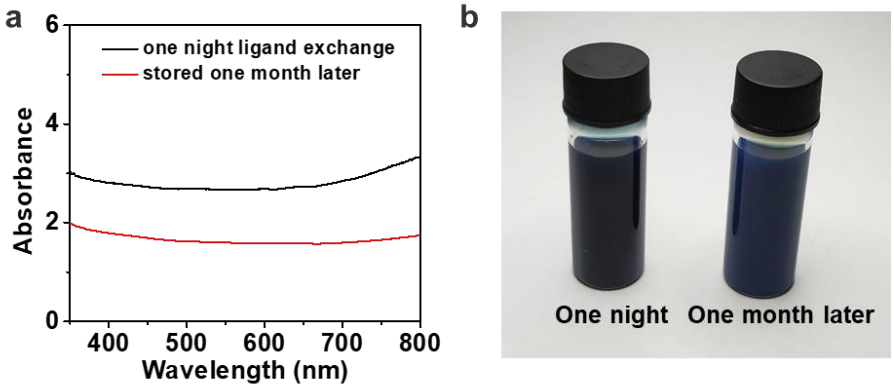

Figure S2. (a) Absorbance spectra of WO_{3-x} nanocrystals in NMP collected from different ligand exchange periods. (b) Photos of the corresponding WO_{3-x} inks.

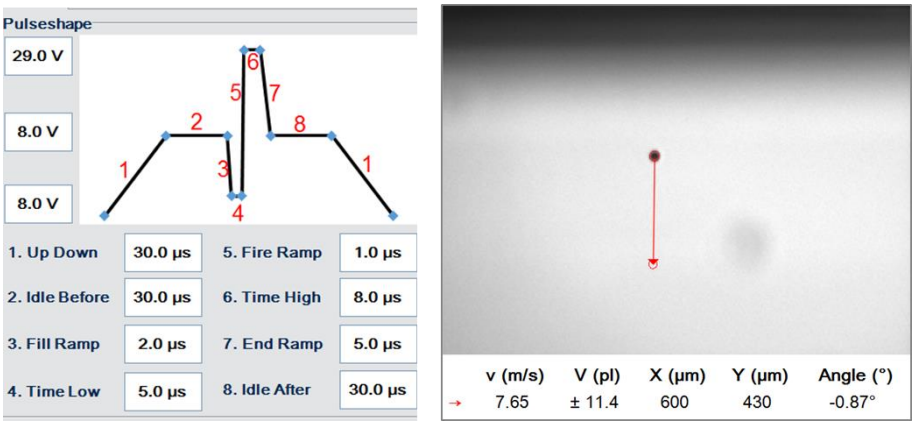

Figure S3. Printing parameters and stroboscopic image of ink droplet jetting from the print head.

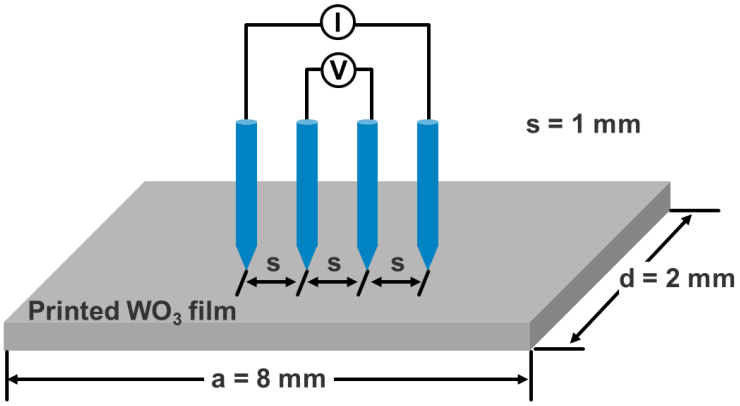

Figure S4. Four-point probe conductivity measurement configuration of WO_{3-x} on bare PET substrate.

The film conductivity σ can be expressed as:[1]

$$\sigma = \frac{I}{VtC}$$

where I and V are the measured current and voltage, t is film thickness, and C is a correction factor. When $d/s = 2$ and $a/d \geq 4$, C is equal to 1.9475.

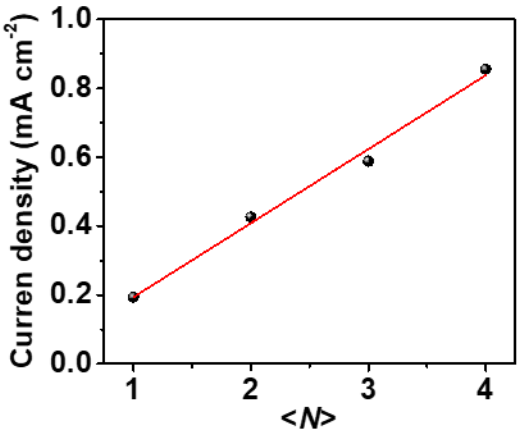

Figure S5. Anodic peak current as a function of the printing pass collected from Figure 2b.

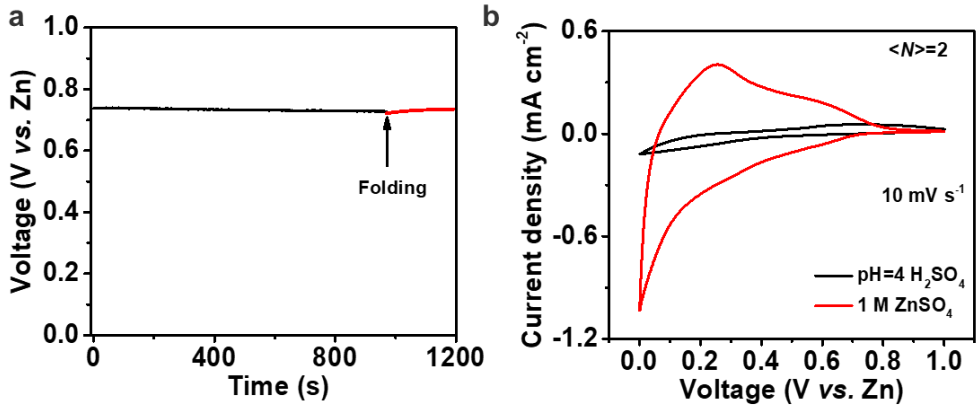

Figure S6. (a) Open-circuit voltage of the assembled electrochromic energy storage device. Note that mechanical folding has nearly no effect. (b) CV curves of the WO_{3-x} electrode with different electrolytes. The pH value of 1 mol L^{-1} $ZnSO_4$ is about 4, so we performed the measurement by using H_2SO_4 solution with pH value at 4 as the electrolytes, and the result indicates proton has a limited effect on the electrochemical properties during the experiment.

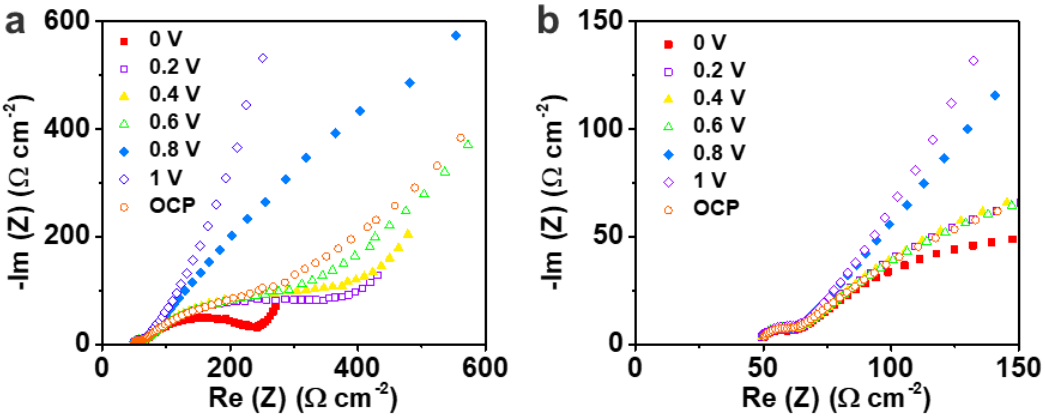

Figure S7. (a) EIS measurement of the device under different voltage. (b) Zoom-in plot of high-frequency region.

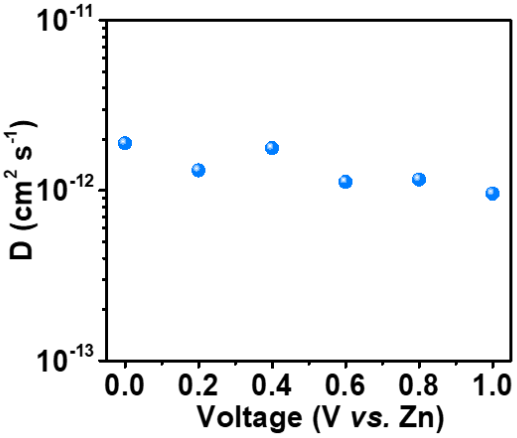

Figure S8. Zinc ion diffusion coefficients collected by potentiostatic intermittent titration technique (PITT).

In a typical PITT measurement, a cell composed of metallic zinc (counter and reference electrode), 1 mol L^{-1} $ZnSO_4$ electrolyte, and printed WO_{3-x} electrode (working electrode) is employed. The diffusion coefficient D of the active material present in the electrode is related to the current i developed from the constant voltage pulses *via* the following formula:[2]

$$D = \frac{\mathrm{d}\ln|i|}{\mathrm{d}t}\frac{4L^2}{\pi^2}$$

where L the characteristic length of the active electrode material.

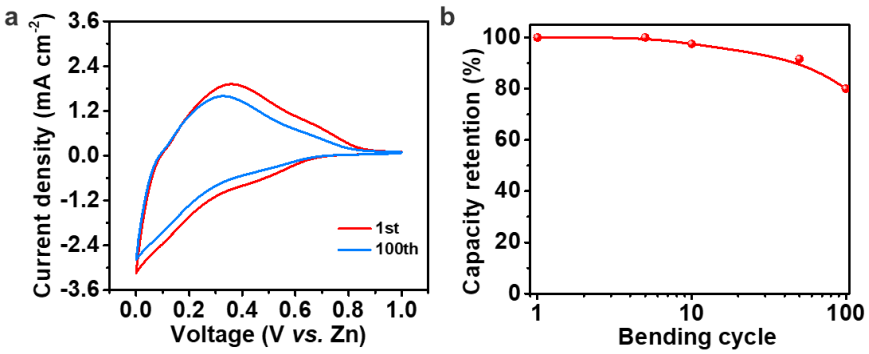

Figure S9. Bending cycle performance with 90° configuration. (a) CV curves at 50 mV s^{-1} after 1st and 100th bending cycle. (b) Long-term bending cycle performance.

Table S2. Overview of inkjet-printed electrochromic electrodes/devices.

Printed Materials	Size (nm)	Concentration	Solvent [a]	Device configuration	Coloration efficiency ($cm^2\ C^{-1}$)	Working voltage (V)	Year & Reference
PANI/PEDOT-silica	200-300	/	PC	Single electrode	/	-2/2	2008[3]
WO_3	200	~4 mg mL^{-1}	Water	WO_3//WO_3	27 @ 700 nm	0.5/2	2012[4]
V_2O_5	~64	/	Water	V_2O_5//V_2O_5	22.3 @ 750 nm	-1.5/1.5	2012[5]
a-WO_3/TiO_2/WO_x	/	0.01 wt%	Water and EtOH	TiO_2-WO_x//ITO	9-530 @ 900 nm	-1/4	2012[6] 2014[7]
WO_3	90	0.5-5 wt%	water and DB	Single electrode	65.5 @ 633 nm	-1.2/1.2	2014[8]
a-WO_3/WO_3	138-182	0.03 wt%	Water and EtOH	Single electrode	4.4 @ 800 nm	-2/2	2015[9]
WO_3, NiO	50-120, 30-50	1 wt%	DB, EG and water	WO_3//NiO	47.3-66.5 @ 633 nm	-2.5/2	2016[10]
WO_3/PEDOT:PSS	50-120	/	DB and water	CeO_2/TiO_2// WO_3/PEDOT:PSS	108.9 @ 633 nm	-2/2	2017[11]
	50-120	/	DB and water	WO_3/PEDOT:PSS/ //ITO	42.1 @ 633 nm	-0.6/0	2018[12]
	50-120	/	DB and water	WO_3/PEDOT:PSS/ Ag//PANI/CNT	75.5 @ 633 nm	0/1.5	2018[13]
	~20	/	Water and EtOH	WO_3/PEDOT:PSS/ //ITO	83.9 @ 650 nm	-1.1/1	2018[14]
WO_{3-x}	**~4**	**100 mg mL^{-1}**	**NMP, IPA or EtOH**	**WO_{3-x} //Zn**	**57.4-97.7 @ 633 nm**	**0/1**	**2020 This work**

[a] Solvent abbreviation: propylene carbonate-PC; diethylene glycol *n*-butyl ether-DB; ethylene glycol-EG.

Vedieo S1. 10 pL additive-free ink droplet jetting process.

Supplementary references

[1] F. M. Smits, *Bell Syst. Tech. J.* **1958**, *37*, 711.

[2] C. J. Wen, B. A. Boukamp, R. A. Huggins, W. Weppner, *J. Electrochem. Soc.* **1979**, *126*, 2258.

[3] G. H. Shim, M. G. Han, J. C. Sharp-Norton, S. E. Creager, S. H. Foulger, *J. Mater. Chem.* **2008**, *18*, 594.

[4] C. Costa, C. Pinheiro, I. Henriques, C. A. T. Laia, *ACS Appl. Mater. Interfaces* **2012**, *4*, 1330.

[5] C. Costa, C. Pinheiro, I. Henriques, C. A. T. Laia, *ACS Appl. Mater. Interfaces* **2012**, *4*, 5266.

[6] P. J. Wojcik, A. S. Cruz, L. Santos, L. Pereira, R. Martins, E. Fortunato, *J. Mater. Chem.* **2012**, *22*, 13268.

[7] P. J. Wojcik, L. Pereira, R. Martins, E. Fortunato, *ACS Comb. Sci.* **2014**, *16*, 5.

[8] M. Layani, P. Darmawan, W. L. Foo, L. Liu, A. Kamyshny, D. Mandler, S. Magdassi, P. S. Lee, *Nanoscale* **2014**, *6*, 4572.

[9] L. Santos, P. Wojcik, J. V. Pinto, E. Elangovan, J. Viegas, L. Pereira, R. Martins, E. Fortunato, *Adv. Electron. Mater.* **2015**, *1*, 1400002.

[10] G. Cai, P. Darmawan, M. Cui, J. Chen, X. Wang, A. L.-S. Eh, S. Magdassi, P. S. Lee, *Nanoscale* **2016**, *8*, 348.

[11] G. Cai, P. Darmawan, X. Cheng, P. S. Lee, *Adv. Energy Mater.* **2017**, *7*, 1602598.

[12] G. Cai, X. Cheng, M. Layani, A. W. M. Tan, S. Li, A. L.-S. Eh, D. Gao, S. Magdassi, P. S. Lee, *Nano Energy* **2018**, *49*, 147.

[13] G. Cai, S. Park, X. Cheng, A. L.-S. Eh, P. S. Lee, *Sci. Technol. Adv. Mater.* **2018**, *19*, 759.

[14] C.-W. Chang-Jian, E.-C. Cho, S.-C. Yen, B.-C. Ho, K.-C. Lee, J.-H. Huang, Y.-S. Hsiao, *Dyes Pigm.* **2018**, *148*, 465.